Nucleation Density and Shape of Submonolayer Two-Dimensional Islands of Diphenyl Dinaphthothienothiophene in Vacuum Deposition

Hattori, Yoshiaki

Kimura, Yoshinari

Kitamura, Masatoshi

(Citation)
Journal of Physical Chemistry C,124(1):1064-1069

(Issue Date)
2020-01-09

(Resource Type)
journal article

(Version)
Accepted Manuscript

Nucleation Density and Shape of Sub-Monolayer Two-Dimensional Islands of Diphenyl Dinaphthothienothiophene in Vacuum Deposition

Yoshiaki Hattori[*]*, Yoshinari Kimura, and Masatoshi Kitamura*[**]

Department of Electrical and Electronic Engineering, Kobe University, 1-1, Rokkodai-cho, Nada-ku, Kobe, 657-8501, Japan

Abstract:

Sub-monolayer two-dimensional (2D) islands of diphenyl dinaphthothienothiophene with various shapes and densities (N) were formed on a SiO_2/Si substrate by controlling substrate temperature and the surface treatment for SiO_2 in vacuum deposition to investigate the growth mechanism based on their morphology. The statistical analysis shows that the 2D islands have complex shapes when N is small, and there is a constant relationship between N and the shape complexity of the 2D islands, regardless of the deposition conditions. Since the surface morphology is determined by diffusion coefficients for admolecules on a substrate surface (D_s) and along the edge of a 2D island (D_{edg}), the relationship between (N, shape complexity) and (D_s, D_{edg}) is studied. The statistical analysis indicates that D_{edg} is almost independent of the surface conditions and is instead determined by interactions with molecules constructing the 2D island. Therefore, D_{edg} is considered as a material-dependent parameter to control the morphology for growing high-quality films in vacuum deposition.

Introduction

The formation of two-dimensional (2D) islands in vapor-phase epitaxy has been studied for metals [1-6] and semiconductors [7-11] to grow high-quality thin films. Scanning tunneling microscopy has shown that the nucleation density (N) and shape of 2D islands depend on substrate temperature (T_s) and/or deposition rate [1-10]. These 2D islands exhibit round,[1] triangular,[2, 8] square,[3] or complicated fractal shapes.[1, 2, 4] To understand their growth mechanism, various models for kinetic Monte Carlo simulations[12-17] and analytical theories[18, 19] have been developed. The primary physical parameters determining morphology are diffusion coefficients for atoms on a substrate surface (D_s) and along the edge of a 2D island (D_{edg}).[12-14] The edge diffusion behavior is particularly important in dynamics, since sites that are stable for atoms dominate the island shape.

In growth of organic molecule films, pentacene, a standard organic semiconductor, is grown on an amorphous oxide substrate in layer-by-layer growth mode,[20-24] as observed in epitaxial growth of metals and semiconductors. However, in contrast to epitaxial growth, weak bonding arises as physical adsorption between a molecule and a substrate. Therefore, the surface conditions of the substrate, such as roughness or surface energy, are additional experimental parameters to consider in growth.[20, 25-32] Since organic molecules actively diffuse on an amorphous substrate, in contrast to atoms in epitaxial growth, organic 2D island has N value of 10^{-1}–10^{2} μm^{-2},[21, 25-30, 33-35] which is smaller than the value of 10^{1}–10^{4} μm^{-2} for epitaxial growth.[1-11] Consequently, larger 2D islands form on a substrate, enabling atomic force microscopy (AFM) investigation.[21-23, 25-31, 33-36] With respect to shape, 2D islands of organic small molecules tend to form randomly on the substrate with distorted round or fractal shapes.[21, 26-30, 33-35, 37-40] This is probably attributed to weak interaction of organic molecules to an amorphous substrate.

Recently, we have found that the surface morphology of thin films of 2,9-diphenyl-dinaphtho[2,3-*b*:2′,3′-*f*]thieno[3,2-*b*]thiophene (DPh-DNTT), which is an elongated organic small molecule similar to pentacene, is strongly influenced by treatment for SiO_2 substrate surfaces compared to deposition of pentacene.[40] Furthermore, 2D islands with a diameter of a few μm form on the substrate under certain conditions, enabling optical microscopy observation. Therefore, DPh-DNTT is considered a favorable material for investigating growth mechanism of organic thin films. Regarding shape for 2D islands, simulation models developed in a previous study demonstrated that the shape complexity is related to the ratio of D_s and D_{edg}.[12-15] However, experimental results providing substantial evidence for this relationship are lacking.

In this paper, the relationship between N and shape complexity of 2D islands consisting of DPh-DNTT molecules is reported to investigate growth mechanism of organic molecules. To examine the influence of substrate temperature (T_s) and surface modification, N and the complexity for 2D islands deposited under various conditions were statistically analyzed. The area (A) and perimeter (P) of 2D islands, measured by optical microscopy, were applied to evaluate the complexity, which is represented as P^2/A.[41] The relationship between (N, P^2/A) and (D_s, D_{edg}) is described. In addition, temperature dependences of D_s and D_{edg} are discussed. Finally, we experimentally demonstrate that the complexity of these 2D islands is governed by D_{edg}.

Experimental Procedures

DPh-DNTT thin films were deposited on Si substrates with thermally grown 90-nm-thick SiO_2 at a pressure of the order of 10^{-4} Pa with a deposition rate of 0.05 Å/s. The deposition rate was monitored using a quartz crystal microbalance. T_s was set from 150°C to 185°C. Before the substrates were mounted, the SiO_2 surface was treated with O_2 plasma, UV-O_3, or HF solution.

Details regarding the O_2 plasma and UV-O_3 surface treatment are given in our previous paper.[42] HF solution was used to chemically etch the SiO_2 surface by a few nanometers. After cleaning by sonication, the substrate was immersed in HF solution diluted to 2.5 vol% with deionized water for 30 s. All surface treatments modified the surface to render it more hydrophilic. For most samples, the RMS roughness of the substrate was less than 0.4 nm. After deposition, the shape and N of the 2D islands were evaluated in the optical microscopic images using digital image processing (**Fig. S1 and S2**, Supporting Information).

Results and discussion

Figure 1 shows typical photographs of 2D islands deposited at different T_s values for O_2 plasma and HF treatment. The nominal film thickness was 1.5 ± 0.3 nm. The values of N and the coverage for each sample are shown in each image. The value of P^2/A indicates the complexity of the 2D island shape, as discussed below. When T_s is high, N is small, and the islands exhibit complex shapes. At a same T_s, N for HF treatment is slightly smaller than that for O_2 plasma treatment, as seen in **Fig. 1**.

Figures 2(a) and **2(b)** show optical microscopy images for 2D islands deposited at 185°C on a SiO_2 surface treated with HF. **Figure 2(a)** presents a dark-field image, and **Fig. 2(b)** displays a polarized image of the same area, acquired with crossed polarizers and a narrow 498-nm band-pass filter. Compared with **Fig. 1(d–f)**, the 2D islands in **Fig. 2(a, b)** have more complicated shapes, exhibiting diphycercal symmetry with the major and minor axes. The two arrows in **Fig. 2(b)** indicate the transmission axis of polarizers. In the polarized image, each 2D island displays a single color, which varies for each island. A 2D island with its major axis parallel to the polarizer axis is not optically observed in the polarizing image. In contrast, a 2D island whose major axis is oriented

45° from the polarizer axis is clearly imaged in a whitish color. Periodical color changes are a typical characteristic of polarization and have been observed in the monolayer growth of organic films.[43, 44] **Figure 2(c)** shows a topological AFM image for the same substrate displayed in **Fig. 2(a, b)**, which more clearly shows the morphology of a 2D island with diphycercal symmetry and a fractal structure with higher resolution. The inset shows cross-sectional profiles along the dotted line in the topological image, indicating an island height of 2.3 nm. The value is close to the length of DPh-DNTT molecule,[40] suggesting that molecules in the 2D islands are aligned vertically with respect to the substrate. These observations suggest that the 2D islands grow in a highly ordered manner on a microscopic scale.

Here, we discuss the 2D island orientation. The previous study reported that the crystal structure of DPh-DNTT is monoclinic.[45] The observed shape with diphycercal symmetry may reflect two crystal axes which make a 90° in monoclinic herringbone structure. If the hypothesis is correct, the two crystal axes possibly correspond to either the long or short island axis, as shown in **Fig. 2(d)**. As mentioned above, 2D islands of pentacene generally grow in a round shape on an amorphous substrate. However, the similar rhombus shapes are observed when the underlying material is crystalline, such as a Si substrate, or when nucleation occurs on the first layer that forms on a thermally oxidized Si substrate.[27, 35, 36] This might indicate a potential similarity in the molecule and crystal packing structure between pentacene and DPh-DNTT thin films.

To quantitatively analyze N for each surface treatment, the N value obtained from optical microscopy images is shown as a function of inverse T_s in **Fig. 3**. N exponentially decreases with increasing T_s regardless of the surface treatment. Although small N values are obtained at high T_s, there is an upper limit of T_s for film formation (**Note S1**, **Fig. S3**, Supporting Information). As shown in **Fig. 1**, N for the HF treatment is smaller than that for O_2 plasma or UV-O_3 treatment. N

is discussed based on D_s playing a critical role in the dynamics of admolecules on a SiO_2 surface. A molecule arriving on a surface randomly migrates until it is adsorbed on an island. Then, the molecule diffuses along the island edge, and locates at a certain site that is stable for the molecule. N generally decreases with increasing D_s. Molecules actively diffuse on a surface at high T_s. Thus, the relationship between T_s and D_s is expressed by the Arrhenius equation:

$$D_s = D_{0,s}\exp(-E_{dif,s}/kT_s) \quad (1)$$

where $D_{0,s}$ is a constant, $E_{dif,s}$ is the activation energy for monomer surface diffusion, and k is Boltzmann constant.[16, 17] The temperature dependence of N in **Fig. 3** is explained by **Eq. (1)**. The different dependences on surface treatment indicate that the HF, O_2 plasma, and UV-O_3 surface treatments enhance admolecule migration, resulting in large D_s values in this order. In contrast, the case with no surface treatment exhibited a small N.[40]

The complexity of 2D island shapes is examined based on A and P. This is because an island with a complex shape has a larger P for a given A, with the nondimensional value P^2/A representing island shape complexity. A large P^2/A indicates a complex shape, and vice versa. A typical example is a perfect circle with $P^2/A = 4\pi$, which is the smallest value for any shape. A and P of the islands were measured from the dark-field optical images using image processing (**Fig. S1**, Supporting Information). Although the resolution of the optical microscopy affects the evaluation for the complicated shape islands such as **Fig. 2**, the all samples were evaluated by the same method as a qualitative evaluation. The error for the complicated shape is discussed in more detail in **Fig. S2**. The P^2/A values shown in **Fig. 1** are averages for the 2D islands. **Figure 4(a)** shows P^2/A as a function of N for various treatments at different T_s values, calculated from optical microscopy images. P^2/A dramatically increases with decreasing N, indicating that islands with

low N values have complex shapes. Notably, the relationship between P^2/A and N is approximately on the same curve regardless of surface treatment.

P^2/A may be related to D_s and D_{edg}. Previous kinetic Monte Carlo simulations demonstrated that 2D islands have a complex shape when D_{edg}/D_s is small. This means that P^2/A is represented by D_{edg}/D_s, where a large P^2/A corresponds to a small D_{edg}/D_s. Moreover, a large N corresponds to a small D_s based on the above-described relationship between N and D_s. Therefore, the vertical and horizontal axes in **Fig. 4(a)** are related to D_{edg}/D_s and D_s, respectively. Namely, **Fig. 4(a)** can be considered as D_{edg}/D_s versus D_s. Since the relationship between P^2/A and N is independent of the surface treatment, the relationship between D_{edg}/D_s and D_s does not depend on the surface treatment. This means that D_{edg} is a function of D_s regardless of the surface treatment. This conclusion is interpreted as follows. Molecules on a substrate diffuse along an island edge and primarily interact with molecules constructing the island rather than with the substrate surface.[41]

Since D_{edg}/D_s is directly related to the shape complexity of 2D islands, we discuss the temperature dependences of D_s and D_{edg}. On the basis of the following discussion, the dependences are qualitatively expressed in **Fig. 4(b)**. Similar to D_s, D_{edg} is given by the Arrhenius equation[16, 17]:

$$D_{edg} = D_{0,edg}\exp(-E_{dif,edg}/kT_s) \qquad (2)$$

where $D_{0,edg}$ is a constant and $E_{dif,edg}$ is the activation energy for edge diffusion. From **Eqs. (1)** and **(2)**, D_s and D_{edg} are expressed by straight lines, as shown in **Fig. 4(b)**. D_{edg} is constant for all three surface treatments and is expressed by a line. D_{edg} is much smaller than D_s because the intermolecular interaction is stronger than that between admolecule and surface. In fact, D_{edg}/D_s values in the range of zero to 10^{-6} have been used in simulation studies.[12] Thus, the line for D_{edg} is placed below the lines for D_s. The slope of the line corresponds to $-E_{dif,edg}/k$, although the actual

value is unknown. The slope for D_s can be determined from the experimentally observed shape complexity. This is because shape complexity is represented by D_{edg}/D_s. As seen in **Fig. 1**, 2D islands observed at high T_s have complex shapes, corresponding to large P^2/A, small D_{edg}/D_s, and large ($\log D_s - \log D_{edg}$) values. In contrast, 2D islands observed at low T_s have compact shapes, corresponding to small ($\log D_s - \log D_{edg}$) values. Thus, D_{edg} is expressed by a line with a gentler slope than that of D_s. Consequently, we conclude that the different shape dependences on T_s arise from the different temperature dependences between D_s and D_{edg}.

The different slopes indicate that $E_{dif,edg} < E_{dif,s}$, which may seem inconsistent with the relationship of $D_{edg} < D_s$. This is because the origin of small D_{edg} is explained as a large interaction between an admolecule and a molecule of a 2D island. The large interaction is reminiscent of a large $E_{dif,edg}$. However, the relationship between the interaction and $E_{dif,edg}$ is not simple. D_s for an amorphous substrate with energy potential fluctuations in this case. An admolecule at a site jumps to another minimal-energy site that randomly arises, resulting in a large D_s.[26] In contrast, edge diffusion ideally occurs with molecules moving from neighbor sites one by one because a 2D island is composed of highly ordered molecules.

This interpretation of shape complexity based on D_{edg}/D_s is applied to the following types of growth: (i) subsequent layers, (ii) other conditions for vacuum deposition, and (iii) other materials. Under the first condition, subsequent layers grow in a layer-by-layer mode after the first layer is completed. In our previous study, the complex-shaped DPh-DNTT 2D islands were observed on a multilayer surface consisting of DPh-DNTT molecules. Moreover, the island density is lower than that of the first layer for both UV-O_3 and O_2 plasma surface treatment.[40] Accordingly, the shape and density can be explained by D_s on the multilayer surface. D_s on a surface consisting of DPh-DNTT molecules is larger than that on a SiO_2 surface. Since D_{edg} is independent of the underlying

material, a large D_s leads to a small D_{edg}/D_s, resulting in complex-shaped 2D islands with low N. The second application is based on the vacuum deposition rate. It has been theoretically[18, 19] and experimentally[10, 26, 29] shown that N increases with increasing deposition rate. Therefore, small 2D islands with round shapes with high N values are expected for a high deposition rate, which can also be explained by a scaling law[15, 16-19]. The third application is growth of other molecules with an elongated structure, including pentacene and DNTT derivative. The similar relationship between N and the shape complexity of 2D islands has been observed for pentacene.[33] On the basis of these examples, the qualitative relationship between N and the shape complexity is most likely a universal phenomenon for the organic materials.

Conclusions

In conclusion, sub-monolayer DPh-DNTT 2D islands with various shapes and N values were formed on a SiO_2/Si substrate by controlling T_s and the surface treatment for SiO_2 to investigate the growth mechanism based on their morphology. The statistical analysis showed that the 2D islands have complex shapes when N is small, regardless of the deposition conditions. This result indicates that it is difficult to completely alter the relationship between N and complexity in the current system. When organic thin films are used for electronic devices such as thin-film transistors, compact 2D islands with small N values are desirable for enhancing carrier transport in the film. Although there is above difficulty, it is possible that an appropriate molecular design enhances edge diffusion along a 2D island to increase D_{edg} potentially. Thus, the experimental results presented in this study indicate the importance of molecular design for device applications.

ASSOCIATED CONTENT

The image analysis, the influene of the resolution of the optical microscopy on the measured P, the coverage of sub-monolayer as a function of T_s, and the effect of coverage on P^2/A are shown in the Supporting Information.

AUTHOR INFORMATION

Corresponding Authors

Email: *hattori@eedept.kobe-u.ac.jp, **kitamura@eedept.kobe-u.ac.jp

ORCID

Yoshiaki Hattori : 0000-0002-5400-8820

Masatoshi Kitamura : 0000-0003-1342-4796

Notes

The authors declare no competing financial interest

ACKNOWLEDGMENT

This work was partly supported by a Leading Initiative for Excellent Young Researchers program from the MEXT in Japan, JSPS KAKENHI Grant Numbers 19H02171, 19K15048, and17H06229, Materials Science Foundation from Hitachi Metals, Research Foundation for the Electrotechnology of Chubu, and Kawanishi Memorial ShinMaywa Education Foundation. The authors would like to thank Nippon Kayaku Co., Ltd. for supplying us DPh-DNTT.

REFERENCES

(1) Tsui, F.; Wellman, J.; Uher, C.; Clarke, R. Morphology Transition and Layer-by-Layer Growth of Rh (111). *Phys. Rev. Lett.* **1996**, *76* (17), 3164.

(2) Busse, C.; Langenkamp, W.; Polop, C.; Petersen, A.; Hansen, H.; Linke, U.; Feibelman, P. J.; Michely, T. Dimer Binding Energies on Fcc (111) Metal Surfaces. *Surf. Sci.* **2003**, *539* (1–3), L560–L566.

(3) Zhang, C.-M.; Bartelt, M. C.; Wen, J.-M.; Jenks, C. J.; Evans, J. W.; Thiel, P. A. Submonolayer Island Formation and the Onset of Multilayer Growth during Ag/Ag (100) Homoepitaxy. *Surf. Sci.* **1998**, *406* (1–3), 178–193.

(4) Cox, E.; Li, M.; Chung, P.-W.; Ghosh, C.; Rahman, T. S.; Jenks, C. J.; Evans, J. W.; Thiel, P. A. Temperature Dependence of Island Growth Shapes during Submonolayer Deposition of Ag on Ag (111). *Phys. Rev. B* **2005**, *71* (11), 115414.

(5) Stroscio, J. A.; Pierce, D. T. Scaling of Diffusion-Mediated Island Growth in Iron-on-Iron Homoepitaxy. *Phys. Rev. B* **1994**, *49* (12), 8522.

(6) Brune, H.; Bromann, K.; Röder, H.; Kern, K.; Jacobsen, J.; Stoltze, P.; Jacobsen, K.; No, J. Effect of Strain on Surface Diffusion and Nucleation. *Phys. Rev. B* **1995**, *52* (20), R14380.

(7) Okada, M.; Muto, A.; Ikeda, H.; Zaima, S.; Yasuda, Y. Nucleation and Growth of Ge on Si (1 1 1) by MBE with Additional Atomic Hydrogen Irradiation Studied by Scanning Tunneling Microscopy. *J. Cryst. Growth* **1998**, *188* (1–4), 119–124.

(8) Harada, Y.; Yamamoto, M.; Baba, T.; Kita, T. Epitaxial Two-Dimensional Nitrogen Atomic Sheet in GaAs. *Appl. Phys. Lett.* **2014**, *104* (4), 041907.

(9) Filimonov, S.; Cherepanov, V.; Hervieu, Y.; Voigtländer, B. Multistage Nucleation of Two-Dimensional Si Islands on Si (111)-7×7 during MBE Growth: STM Experiments and Extended Rate-Equation Model. *Physl Rev. B* **2007**, *76* (3), 035428.

(10) Joyce, B. A.; Vvedensky, D. D.; Bell, G. R.; Belk, J. G.; Itoh, M.; Jones, T. S. Nucleation and Growth Mechanisms during MBE of III–V Compounds. *Mat. Sci. Eng.: B* **1999**, *67* (1–2), 7–16.

(11) Nikiforov, A. I.; Timofeev, V. A.; Teys, S. A.; Gutakovsky, A. K.; Pchelyakov, O. P. Initial Stage Growth of Ge x Si 1- x Layers and Ge Quantum Dot Formation on Ge x Si 1- x Surface by MBE. *Nanoscale Res. Lett.* **2012**, *7* (1), 561.

(12) Saito, Y. Two-Dimensional Nucleation with Edge and Corner Diffusions. *Journal of the Physical Society of Japan* **2003**, *72* (8), 2008–2014.

(13) Pimpinelli, A.; Ferrando, R. Reentrant Morphological Instability of Epitaxial Islands. *Phys. Rev. B* **1999**, *60* (24), 17016.

(14) Bales, G. S.; Chrzan, D. C. Transition from Compact to Fractal Islands during Submonolayer Epitaxial Growth. *Phys. Rev. Lett.* **1995**, *74* (24), 4879.

(15) Bales, G. S.; Chrzan, D. C. Dynamics of Irreversible Island Growth during Submonolayer Epitaxy. *Phys. Rev. B* **1994**, *50* (9), 6057.

(16) Caspersen, K. J.; Stoldt, C. R.; Layson, A. R.; Bartelt, M. C.; Thiel, P. A.; Evans, J. W. Morphology of Multilayer Ag/Ag (100) Films versus Deposition Temperature: STM Analysis and Atomistic Lattice-Gas Modeling. *Phys. Rev. B* **2001**, *63* (8), 085401.

(17) Caspersen, K. J.; Stoldt, C. R.; Layson, A. R.; Bartelt, M. C.; Thiel, P. A.; Evans, J. W. Morphology of Multilayer Ag/Ag (100) Films versus Deposition Temperature: STM Analysis and Atomistic Lattice-Gas Modeling. *Phys. Rev. B* **2001**, *63* (8), 085401.

(18) Venables, J. A.; Spiller, G. D. T.; Hanbucken, M. Nucleation and growth of thin films. *Rep. Prog. Phys.* **1984**, *47* (4), 399–459.

(19) Bartelt, M. C.; Evans, J. W. Scaling Analysis of Diffusion-Mediated Island Growth in Surface Adsorption Processes. *Phys. Rev. B* **1992**, *46* (19), 12675.

(20) Drummy, L. F.; Martin, D. C. Thickness-Driven Orthorhombic to Triclinic Phase Transformation in Pentacene Thin Films. *Adv. Mater.* **2005**, *17* (7), 903–907.

(21) Guo, D.; Ikeda, S.; Saiki, K. Modified Bimodal Growth Mechanism of Pentacene Thin Films at Elevated Substrate Temperatures. *J. Phys. Condens. Matter* **2010**, *22* (26), 262001.

(22) Cheng, H.-L.; Mai, Y.-S.; Chou, W.-Y.; Chang, L.-R.; Liang, X.-W. Thickness-Dependent Structural Evolutions and Growth Models in Relation to Carrier Transport Properties in Polycrystalline Pentacene Thin Films. *Adv. Funct. Mater.* **2007**, *17* (17), 3639–3649.

(23) Nickel, B.; Barabash, R.; Ruiz, R.; Koch, N.; Kahn, A.; Feldman, L. C.; Haglund, R. F.; Scoles, G. Dislocation Arrangements in Pentacene Thin Films. *Phys. Rev. B* **2004**, *70* (12), 125401.

(24) Shtein, M.; Mapel, J.; Benziger, J. B.; Forrest, S. R. Effects of Film Morphology and Gate Dielectric Surface Preparation on the Electrical Characteristics of Organic-Vapor-Phase-Deposited Pentacene Thin-Film Transistors. *Appl. Phys. Lett.* **2002**, *81* (2), 268–270.

(25) Yang, S. Y.; Shin, K.; Park, C. E. The Effect of Gate-Dielectric Surface Energy on Pentacene Morphology and Organic Field-Effect Transistor Characteristics. *Adv. Funct. Mater.* **2005**, *15* (11), 1806–1814.

(26) Ribič, P. R.; Kalihari, V.; Frisbie, C. D.; Bratina, G. Growth of Ultrathin Pentacene Films on Polymeric Substrates. *Phys. Rev. B* **2009**, *80* (11), 115307.

(27) Ruiz, R.; Nickel, B.; Koch, N.; Feldman, L. C.; Haglund, R. F.; Kahn, A.; Scoles, G. Pentacene Ultrathin Film Formation on Reduced and Oxidized Si Surfaces. *Phys. Rev. B* **2003**, *67* (12), 12506.

(28) Kalb, W.; Lang, P.; Mottaghi, M.; Aubin, H.; Horowitz, G.; Wuttig, M. Structure–Performance Relationship in Pentacene/Al2O3 Thin-Film Transistors. *Synth. Met.* **2004**, *146* (3), 279–282.

(29) Pratontep, S.; Nüesch, F.; Zuppiroli, L.; Brinkmann, M. Comparison between Nucleation of Pentacene Monolayer Islands on Polymeric and Inorganic Substrates. *Phys. Rev. B* **2005**, *72* (8), 085211.

(30) Killampalli, A. S.; Engstrom, J. R. Nucleation of Pentacene Thin Films on Silicon Dioxide Modified with Hexamethyldisilazane. *Appl. Phys. Lett.* **2006**, *88* (14), 143125.

(31) Kelley, T. W.; Boardman, L. D.; Dunbar, T. D.; Muyres, D. V.; Pellerite, M. J.; Smith, T. P. High-Performance OTFTs Using Surface-Modified Alumina Dielectrics. *J. Phys. Chem. B* **2003**, *107* (24), 5877–5881.

(32) Kelley, T. W.; Boardman, L. D.; Dunbar, T. D.; Muyres, D. V.; Pellerite, M. J.; Smith, T. P. High-Performance OTFTs Using Surface-Modified Alumina Dielectrics. *J. Phys. Chem. B* **2003**, *107* (24), 5877–5881.

(33) Stadlober, B.; Haas, U.; Maresch, H.; Haase, A. Growth Model of Pentacene on Inorganic and Organic Dielectrics Based on Scaling and Rate-Equation Theory. *Phys. Rev. B* **2006**, *74* (16), 165302.

(34) Tejima, M.; Kita, K.; Kyuno, K.; Toriumi, A. Study on the Growth Mechanism of Pentacene Thin Films by the Analysis of Island Density and Island Size Distribution. *Appl. Phys. Lett.* **2004**, *85* (17), 3746–3748.

(35) Wang, S. D.; Dong, X.; Lee, C. S.; Lee, S. T. Molecular Orientation and Film Morphology of Pentacene on Native Silicon Oxide Surface. *J. Phys. Chem. B* **2005**, *109* (20), 9892–9896.

(36) Zu Heringdorf, F.-J. M.; Reuter, M. C.; Tromp, R. M. Growth Dynamics of Pentacene Thin Films. *Nature* **2001**, *412* (6846), 517.

(37) Breuer, T.; Karthäuser, A.; Klemm, H.; Genuzio, F.; Peschel, G.; Fuhrich, A.; Schmidt, T.; Witte, G. Exceptional Dewetting of Organic Semiconductor Films: The Case of Dinaphthothienothiophene (DNTT) at Dielectric Interfaces. *ACS Appl. Mater. Interfaces* **2017**, *9* (9), 8384–8392.

(38) Jung, M.-C.; Leyden, M. R.; Nikiforov, G. O.; Lee, M. V.; Lee, H.-K.; Shin, T. J.; Takimiya, K.; Qi, Y. Flat-Lying Semiconductor–Insulator Interfacial Layer in DNTT Thin Films. *ACS Appl. Mater. Interfaces* **2015**, *7* (3), 1833–1840.

(39) Chang, H.; Deng, Y.; Geng, Y.; Wang, T.; Yan, D. Effect of the Initial Stage of Film Growth on Device Performance of Organic Transistors Based on Dinaphtho [2, 3-b: 2′, 3′-f] Thieno [3, 2-b] Thiophene (DNTT). *Org. Electron.* **2015**, *22*, 86–91.

(40) Hattori, Y.; Kimura, Y.; Yoshioka, T.; Kitamura, M. The Growth Mechanism and Characterization of Few-Layer Diphenyl Dinaphthothienothiophene Films Prepared by Vacuum Deposition. *Org. Electron.* **2019**, *74*, 245–250.

(41) Attneave, F. Physical Determinants of the Judged Complexity of Shapes. *J. Exp. Psychol.* **1957**, *53* (4), 221.

(42) Kitani, A.; Kimura, Y.; Kitamura, M.; Arakawa, Y. Threshold Voltage Control in Dinaphthothienothiophene-Based Organic Transistors by Plasma Treatment: Toward Their Application to Logic Circuits. *Jpn. J. Appl. Phys.* **2016**, *55* (3S2), 03DC03.

(43) Cho, J.; Mori, T. Low-Temperature Band Transport and Impact of Contact Resistance in Organic Field-Effect Transistors Based on Single-Crystal Films of Ph-BTBT-C_{10}. *Phys. Rev. Appl.* **2016**, *5* (6), 064017.

(44) Hamai, T.; Arai, S.; Minemawari, H.; Inoue, S.; Kumai, R.; Hasegawa, T. Tunneling and Origin of Large Access Resistance in Layered-Crystal Organic Transistors. *Phys. Rev. Appl.* **2017**, *8* (5), 054011.

(45) Kang, M. J.; Miyazaki, E.; Osaka, I.; Takimiya, K.; Nakao, A. Diphenyl Derivatives of Dinaphtho [2, 3-b: 2′, 3′-f] Thieno [3, 2-b] Thiophene: Organic Semiconductors for Thermally Stable Thin-Film Transistors. *ACS Appl. Mater. Interfaces* **2013**, *5* (7), 2331–2336.

FIGURES

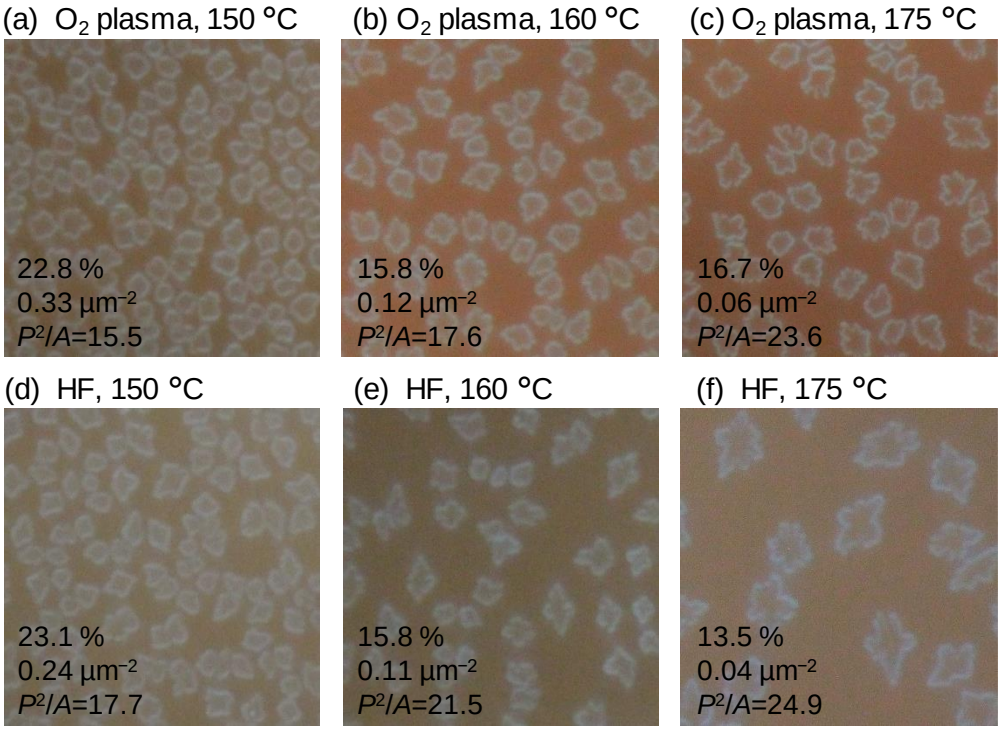

Figure 1: Dark-field optical microscopy of 2D islands deposited on the SiO_2/Si substrates treated with O_2 plasma **(a–c)** and HF **(d–f)** at different T_s values. The coverage, N, and average P^2/A, which indicates the shape complexity, are shown in each image. When T_s is high, complex-shaped islands form with low N values. The N value for the HF treatment is slightly lower than that for the O_2 plasma treatment at the same T_s. The size of each image is 20 × 20 µm.

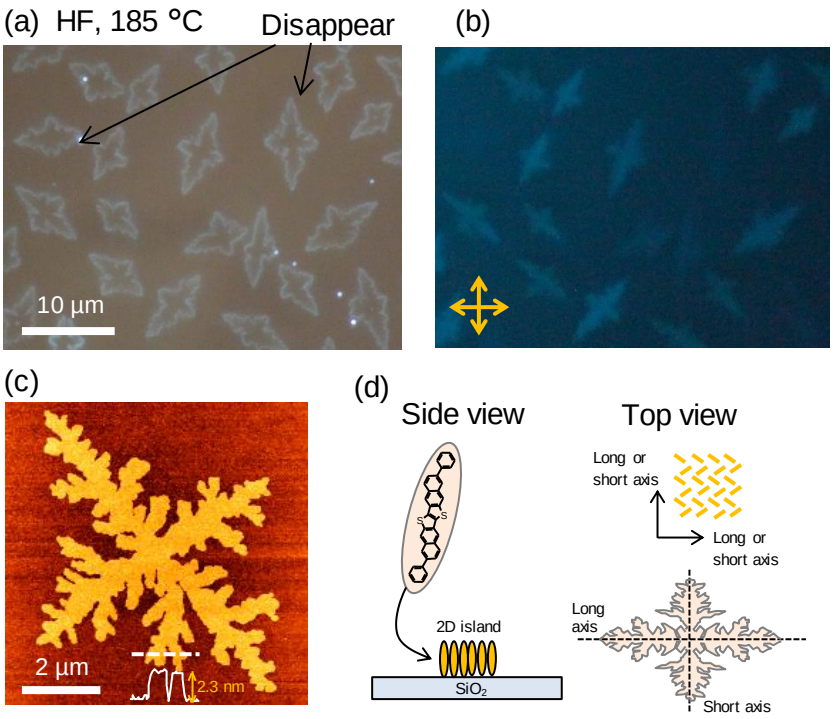

Figure 2: Dark-field optical microscopy **(a)** and polarized imaging with 498-nm crossed polarizers **(b)** of 2D islands deposited at 185°C on an HF-treated SiO_2/Si substrate. The polarized image shows the same area presented in **(a)**. The colors of the islands in the polarized image differ, although the color is constant for each island. The different colors may reflect the crystallinity orientation of the islands. Panel **(c)** presents a topological AFM image of a 2D island for the same substrate displayed in **(a, b)**, exhibiting diphycercal symmetry with a fractal structure. These images suggest that the 2D islands grow with a highly ordered microscopic structure. Panel **(d)** shows the possible crystal structure.

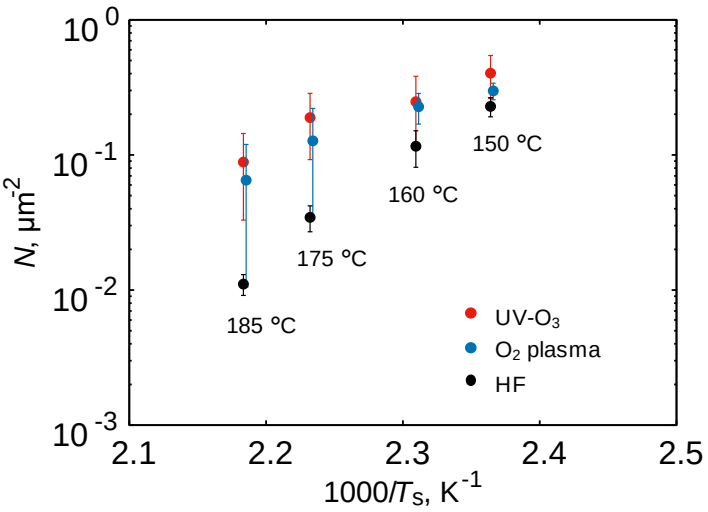

Figure 3: N as a function of the inverse of T_s for various surface treatments. N decreases exponentially as T_s increases, regardless of the surface treatment. Each datapoint is the average N value for more than three samples, and the error bar shows the standard deviation.

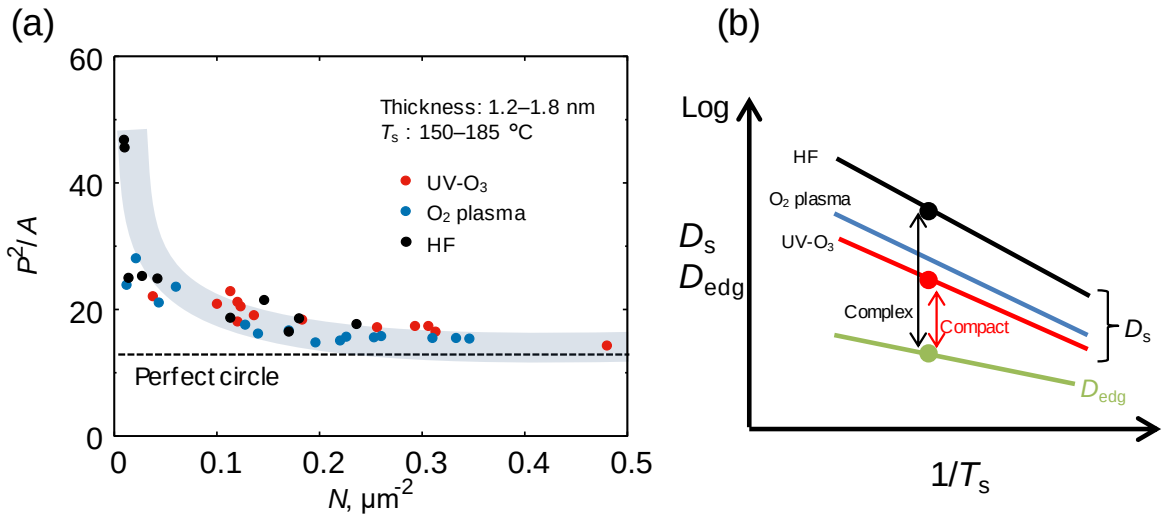

Figure 4: Relationship between N and the shape complexity of 2D islands for various surface treatments at different T_s values **(a)**. P^2/A indicates the complexity. Each datapoint represents the average N and P^2/A values obtained from more than 50 2D islands. The A and P values of each 2D island were measured using image processing (**Fig. S1**, Supporting Information). Since the horizontal and vertical axes in **(a)** can be related to D_s and D_{edg}/D_s, respectively, the T_s dependence of D_s and D_{edg} can be qualitatively predicted, as shown in **(b)**.

TOC Graphic

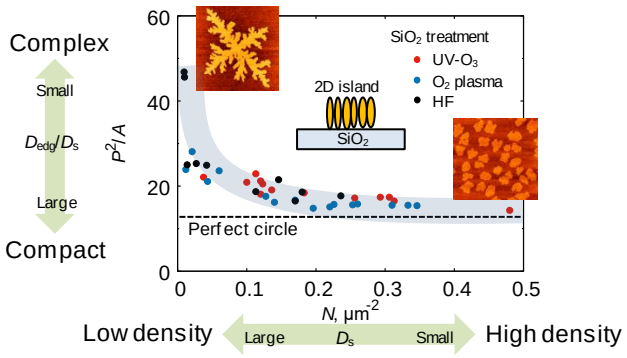
Complex
Small
D_{edg}/D_s
Large
Compact
P^2/A
60
40
20
0
0
0.1
0.2
0.3
0.4
0.5
N, μm^{-2}
SiO_2 treatment
UV-O_3
O_2 plasma
HF
2D island
SiO_2
Perfect circle
Low density
Large
D_s
Small
High density

Supporting Information

Nucleation Density and Shape of Sub-Monolayer Two-Dimensional Islands of Diphenyl Dinaphthothienothiophene in Vacuum Deposition

Yoshiaki Hattori[*]*, Yoshinari Kimura, and Masatoshi Kitamura*[**]

Department of Electrical and Electronic Engineering, Kobe University, 1-1, Rokkodai-cho, Nada-ku, Kobe, 657-8501, Japan

[*]hattori@eedept.kobe-u.ac.jp, [**]kitamura@eedept.kobe-u.ac.jp

Note S1: The effect of the desorption.

Desorption occurs when T_s is high. **Figure S3** shows the coverage of sub-monolayer islands on an O_2-plasma-treated SiO_2/Si substrate as a function of T_s. The nominal thickness is 1.8 nm. The coverage decreases with increasing T_s due to desorption. The upper limit of T_s for film formation is approximately 190°C. Therefore, the coverage and A for each datapoint in **Fig. 4** differ.

For a fairer evaluation, the shape complexity must be assessed for equal A or coverage values. However, it is difficult to control each parameter independently. Therefore, the effect of coverage on the obtained relationship was investigated. **Figure S4** presents P^2/A as a function of N for O_2 plasma treatment at various T_s values, where the coverage is indicated by the color of the datapoints. Since the relationship between complexity and N is based on datapoints with different coverages, the evaluation of complexity is essentially independent of island size, allowing further investigations of D_s and D_{edg}.

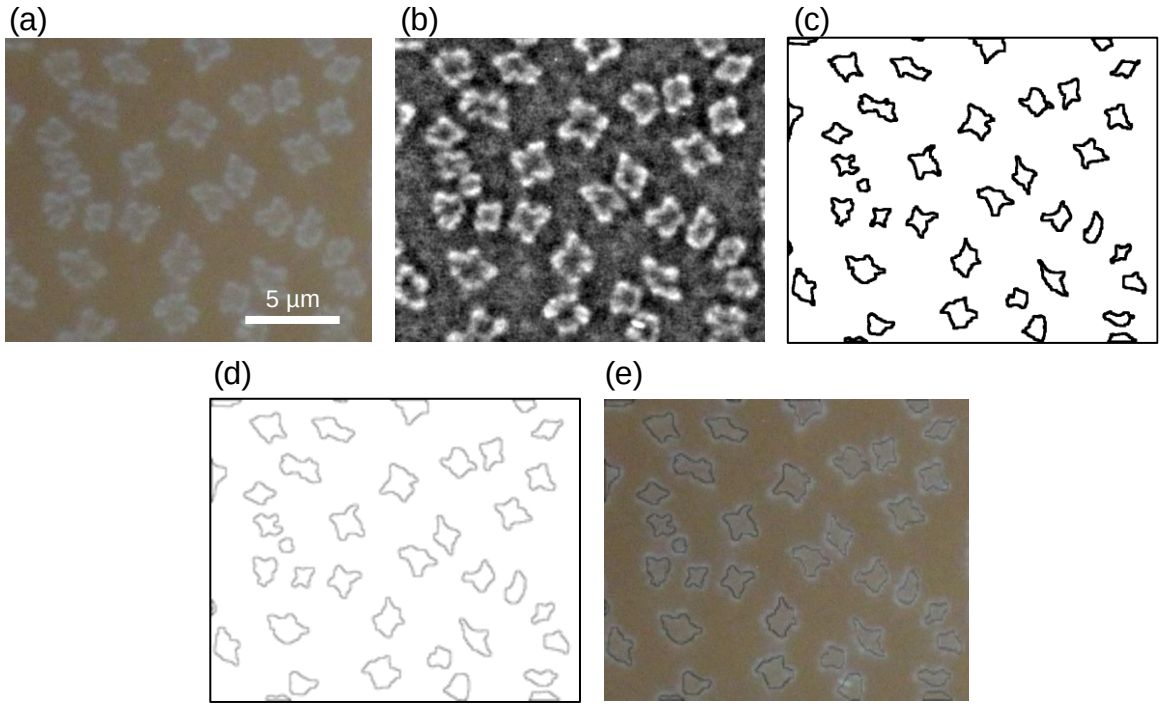

Figure S1: Analysis of images. The obtained photograph (**a**) are converted into grayscale image using blue values (**b**). The outlines of the 2D islands are extracted from the binarized image (**c**). After the bold outlines are thinned using the erosion and dilation functions in the image processing appropriately (**d**), P and A of a 2D island are measured. The image (**e**) shows the comparison of the extracted thin outlines in the original image, indicating the validity of the analysis.

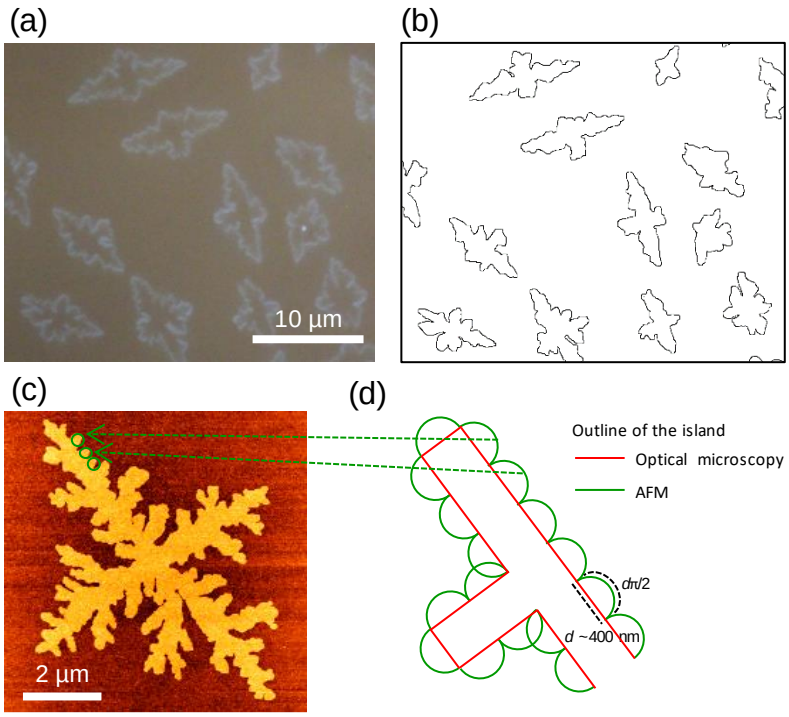

Figure S2: The influence of the resolution of the optical microscopy on the measured *P*. (**a**) and (**b**) show the complicated fractal-shape 2D islands of the optical microscopy image and analyzed outlines, respectively. The image (**c**) shows a topological AFM image of the 2D island for the same substrate displayed in (**a**). Thus, the 2D islands in (**a**) should have the similar structure. From the comparison, the small branches with a length of ~400 nm, indicated by the green circles in (**c**) are not detected in the optical image, which results in reduction of *P*. Panel (**d**) show the model for the complicated 2D island to estimate the error. The red and green lines are the outline of part of the island for the optical microscopy and AFM, respectively. The semicircles with a diameter (*d*) of 400 nm represent the small branches. The length of green line is approximately 1.57 times longer than that of the red line due to the small branches. Therefore, actual P^2/A values for the 2D islands which have the small branches are predicted to be about 2.46 times larger than the plots in **Fig. 4(a)**. The relevant islands form in the case of $N < \sim 0.1$ μm^{-2}. It is expected that P^2/A for low N increases more rapidly than in **Fig. 4(a)**.

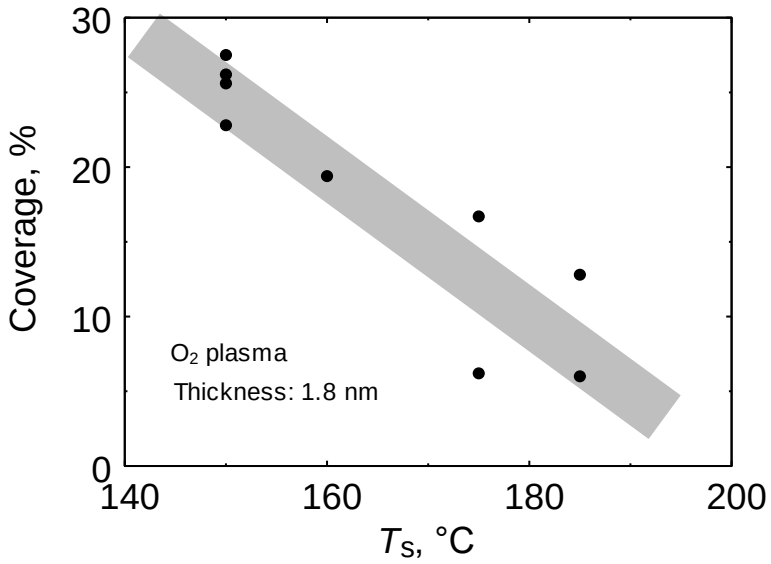

Figure S3: Sub-monolayer coverage on an O_2-plasma-treated SiO_2/Si substrate as a function of T_s for a nominal thickness of 1.8 nm. Desorption occurs at high T_s values.

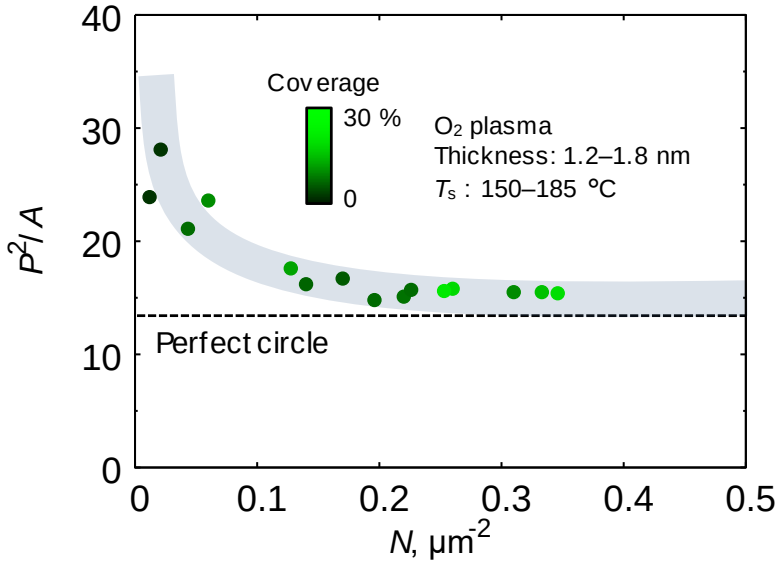

Figure S4: P^2/A as a function of N for O_2 plasma treatment at various T_s values. The shape becomes more complex for smaller N values. The color of each plot indicates sample coverage. Since the relationship between complexity and N is based on datapoints with different coverage values, the complexity evaluation is essentially independent of island size.